Chinese Journal of Aeronautics, 2013,26(3): 777–790

Chinese Society of Aeronautics and Astronautics
& Beihang University

Chinese Journal of Aeronautics

cja@buaa.edu.cn
www.sciencedirect.com

# Design of face-hobbed spiral bevel gears with reduced maximum tooth contact pressure and transmission errors

**Vilmos Simon** *

*Budapest University of Technology and Economics, Faculty of Mechanical Engineering, Department for Machine Design, Műegyetem rkp. 3, H-1111 Budapest, Hungary*

Received 4 September 2012; revised 15 October 2012; accepted 16 January 2013
Available online 16 May 2013

**KEYWORDS**

Ease-off;
Face-hobbed spiral bevel gears;
Load distribution;
Transmission errors;
Gear teeth

**Abstract** The aim of this study is to define optimal tooth modifications, introduced by appropriately chosen head-cutter geometry and machine tool setting, to simultaneously minimize tooth contact pressure and angular displacement error of the driven gear (transmission error) of face-hobbed spiral bevel gears. As a result of these modifications, the gear pair becomes mismatched, and a point contact replaces the theoretical line contact. In the applied loaded tooth contact analysis it is assumed that the point contact under load is spreading over a surface along the whole or part of the ''potential'' contact line. A computer program was developed to implement the formulation provided above. By using this program the influence of tooth modifications introduced by the variation in machine tool settings and in head cutter data on load and pressure distributions, transmission errors, and fillet stresses is investigated and discussed. The correlation between the ease-off obtained by pinion tooth modifications and the corresponding tooth contact pressure distribution is investigated and the obtained results are presented.



## 1. Introduction

Face-hobbed spiral bevel gears are widely applied in helicopters and automobiles for transmitting rotation and torque. The most important criteria for the quality of meshing of gears are the transmission error, the proper location of bearing contact, and the maximum tooth contact pressure. The aim of this study is to reduce the maximum tooth contact pressure and transmission errors in face-hobbed spiral bevel gears.

Since many decades, numerous authors have carried out many studies about representation and design of spiral bevel and hypoid gears cut by face-milling method. On the contrary, about gear cut by continuous indexing process, very few works are available. Litvin described the generality of the face-hobbing cutting process and applied it to spiral bevel gears.[1] By Litvin et al.[2] a method is proposed for the direct determination of relations between the pitch cone angles and spiral angles in hypoid gears with face-hobbed teeth of uniform depth. The geometry of tooth surface of spiral bevel gears in Klingelnberg cyclo-palloid system is described and a method for the

* Tel.: +36 1 463 1183.
E-mail address: simon.vilmos@gszi.bme.hu.

Peer review under responsibility of Editorial Committee of CJA.

Production and hosting by Elsevier


http://dx.doi.org/10.1016/j.cja.2013.05.005

**Nomenclature**

| | |
|---|---|
| $e$ | radial machine-tool setting, m |
| $e_n(z_D)$ | composite tooth error, m |
| $h_d$ | tilt distance from tilt center to reference plane of head-cutter, m |
| $i_{g1}$, $i_{g2}$ | ratios of roll in the generation of pinion and gear tooth-surfaces, respectively |
| $N_1$, $N_2$ | numbers of pinion and gear teeth, respectively |
| $p_{max}$ | maximum tooth contact pressure, Pa |
| $r_{prof}$ | radius of circular cutting edge, m |
| $r_{t0}$ | radius of the head-cutter, m |
| $s$ | geometrical separation of tooth surfaces, m |
| $T$ | transmitted torque, N·m |
| $u$ | coordinate of the straight-lined cutter blade profile point, m |
| $x_{ep}$, $z_{ep}$ | coordinates of the center of the circular cutting edge, m |
| $w$ | total tooth deflection, m |
| $\alpha$ | profile angle of straight-lined cutting edge, (°) |
| $\beta_F$ | load distribution factor |
| $\delta_{01}$, $\delta_{02}$ | pitch angles of the pinion and the gear, respectively, (°) |
| $\Delta e$ | radial machine-tool setting variation, m |
| $\Delta F$ | concentrated load acting in the midpoint of the segment, N |
| $\Delta i_{g1}$ | roll ratio variation |
| $\Delta r_{t0}$ | difference in head-cutter radii, m |
| $\Delta y_n$ | composite displacement of contacting surfaces, m |
| $\Delta\Phi_2$ | angular displacement of the driven gear, (°) |
| $\Phi_1$, $\Phi_2$ | rotational angles of the pinion and the gear in mesh, (°) |
| $\Phi_{10}$, $\Phi_{20}$ | initial rotational angles of the pinion and the gear in mesh, (°) |
| $\gamma$ | initial setting angle of head-cutter axis, (°) |
| $\eta_i$ | initial setting angle of head-cutter, (°) |
| $v$ | coordinate of the circular cutter blade profile point, (°) |
| $\kappa$ | tilt angle of cutter spindle with respect to cradle rotation axis, (°) |
| $\mu$ | swivel angle of cutter tilt, (°) |
| $\omega^{(c)}$ | angular velocity of the imaginary generating crown gear, 1/s |
| $\omega^{(t)}$ | angular velocity of the head-cutter, 1/s |
| $\omega^{(1)}$, $\omega^{(2)}$ | angular velocities of the pinion and the gear in mesh, 1/s |
| $\rho_c$ | radius of the rolling circle of the imaginary generating crown gear, m |
| $\rho_t$ | radius of the rolling circle of the head-cutter, m |
| $\sigma_{fil.max(g)}$, $\sigma_{fil.max(p)}$ | maximum fillet stresses in the gear and in the pinion, Pa |
| $\xi_i$ | offset angle of cutter blade, (°) |

inspection of this type of spiral bevel gears is proposed in Ref. 3. The paper published by Kawasaki et al.[4] contains the design method, tooth contact analysis, and the investigation of the influence of assembly errors on the paths of contact and transmission errors in the case of Klingelnberg spiral bevel gears with small spiral angles. The manufacturing of large-sized spiral bevel gears in a Klingelnberg cyclo-palloid system using multi-axis control and multi-tasking machine tool is presented by Kawasaki.[5] Kato and Kubo[6] developed a calculation procedure to determine the tooth bearing and transmission errors of the gears obtained from cutters with different diameters and to clarify the quantitative effects of the cutter diameter on the gear performance. Procedure to obtain the correction values of machine settings for tooth surface modification in the case of face hobbing and the construction of the corresponding prototype gear cutting machine is presented in Ref. 7. The basis of the new face-hobbing method, presented by Stadtfeld,[8] is a cutter system that uses an outside and an inside blade per blade group only and has an equal spacing between all blades. Lelkes et al.[9] proposed a flexible parameter variation method for tooth-surface and contact simulation of the cyclo-palloid spiral bevel gear and discussed the influences of cutting parameters on the result of tooth contact analysis. Fan[10] presented the theory of the Gleason face-hobbing process, who later presented a generic model of tooth surface generation for spiral bevel and hypoid gears produced by face milling and face hobbing processes conducted on freeform CNC hypoid gear generators.[11] The same author in Ref. 12 presented a polynomial representation of the universal motions of machine tool settings on CNC machines. A mathematical model for the universal hypoid generator that can simulate all primary face-hobbing and face-milling processes for spiral bevel and hypoid gears is presented by Shih et al.[13] Shih and Fong[14] proposed a flank modification methodology for face hobbing spiral bevel gear and hypoid gears, based on the ease-off topography of the gear drive. A novel ease-off flank modification methodology for spiral bevel and hypoid gears made by a modern Cartesian-type hypoid gear generator was proposed in Ref. 15. Vimercati[16] presented a mathematical model able to represent tooth surfaces of a complex gear drive: hypoid gears cut by face-hobbing method. Zhang and Wu[17] presented a systematic approach for the determination of complete tooth geometry of hypoid and spiral bevel gears that are generated by face-hobbing process.

Methods for load and stress distribution calculations in face-milled spiral bevel and hypoid gears were presented in Refs. 18–35. Wilcox[18] in his paper outlined the general theory for calculating stresses in spiral bevel and hypoid gears using flexibility matrix method in combination with the finite element method. Bibel et al.[19] applied the FEM to establish the model of tooth contact of spiral bevel gears by using gap elements. The loaded tooth contact analysis predicting the motion error of spiral bevel gear sets, by applying influence matrices, was presented by Gosselin et al.[20] Handschuh and Bibel[21] analytically and experimentally rolled through mesh a spiral bevel gearset to investigate the tooth bending stress by finite element method. The research reported in paper[22] presented a concept of flexibility tensor by which the flexibility factor in arbitrary directions can be obtained, used to solve the contact problem with friction. In the simulation of the manufacturing process of spiral bevel gears, Linke et al.[23] presented a method that takes into account any additional

motions mapped in the process-independent mathematical model of the generating process. This study demonstrated how such additional motions influence the meshing and stress conditions. Vogel et al.[24] proposed a new methodology for TCA by using sensitivities of tooth contact properties regarding arbitrary machine settings. Fang et al.[25] considered the edge contact in loaded tooth contact analysis. Litvin et al.[26] developed an integrated computerized approach for the design and stress analysis of spiral bevel gears with low levels of noise and vibration and increased endurance. De Vaujany et al.[27] presented a numerical tool that simulates the loaded meshing of spiral bevel gears and experimental tests carried out on a real helicopter gear box. Tooth surface contact stress, maximum tensile bending stress and maximum compressive bending stress were investigated by using loaded tooth contact analysis and finite element method in Ref. 28. An approach was proposed by Schlecht et al.[29] for determining the local load capacity in the early development of spiral bevel and hypoid gears under the action of load spectra. Wang et al.[30] used the finite element method to analyze the dynamic responses of gear transmission, surface contact stress, and root bending stress of a spiral bevel gear pair. In Refs. 31–33 a new approach for the computerized simulation of load distribution in mismatched spiral bevel and hypoid gears was presented.

Only a few references can be found on load and stress distribution calculations in face-hobbed spiral bevel and hypoid gears. An advanced contact solver that, using a hybrid method combining finite element technique with semianalytical solutions is applied by Piazza and Vimercati[34] to carry out both contact analysis under light or heavy loads and stress tensile calculation in aerospace face-hobbed spiral bevel gears. Saiki et al.[35] proposed an innovative loaded tooth contact analysis method for lapped hypoid gears directly using the measured tooth flanks at each manufacturing step including milling and hobbing process. Ref. 36 presents the numerical procedure to simulate the loaded behavior of the hypoid gear manufactured by face-hobbing cutting process. Loaded contact patterns and transmission error of both face-milled and face-hobbed spiral bevel and hypoid gears are computed by enforcing the compatibility and equilibrium conditions of the gear mesh in Ref. 37 published by Kolivand and Kahraman. Kolivand and Kahraman[38] proposed a practical methodology based on easy-off topography for loaded tooth contact analysis of face-milled and face-hobbed hypoid gears having both local and global deviations. Kawasaki and Tsuji[39] investigated the tooth contact patterns of large-sized cyclo-palloid spiral bevel gears both analytically and experimentally. Hotait et al.[40] investigated experimentally and theoretically the impact of misalignments on root stresses of hypoid gear sets.

In theory, truly conjugate face-hobbed spiral bevel gears have line contacts. In order to reduce the tooth contact pressure and the transmission errors, and to decrease the sensitivity of the gear pair to errors in tooth surfaces and to the relative positions of the mating members, a set of carefully chosen modifications is usually applied to the teeth of one or both mating gears. As a result of these modifications, the spiral bevel gear pair becomes "mismatched", and a point contact replaces the theoretical line contact. In practice, these modifications are usually introduced by applying the appropriate machine tool setting for the manufacture of the pinion and the gear, or by using a head cutter with an optimized profile.

The aim of this study is to determine the optimal tooth modifications in face-hobbed spiral bevel gears in order to reduce maximum tooth contact pressure and transmission errors. The optimal tooth modifications are introduced into the pinion teeth by appropriate variation in the head-cutter geometry and in machine tool settings. In the applied loaded tooth contact analysis it is assumed that the point contact under load is spreading over a surface along the "potential" contact line, whose line is made up of the points of the mating tooth surfaces in which the separations of these surfaces are minimal, instead of assuming the usually applied elliptical contact area. The separations of contacting tooth surfaces are calculated by applying the full theory of tooth surface generation in face-hobbed spiral bevel gears. The bending and shearing deflections of gear teeth, the local contact deformations of mating surfaces, gear body bending and torsion, the deflections of supporting shafts, and the manufacturing and alignment errors of mating members are included. The tooth deflections of the pinion and gear teeth are calculated by the finite element method. As the equations governing the load sharing among the engaged tooth pairs and the load distribution along the tooth face are nonlinear, an approximate and iterative technique is used to solve this system of equations. A computer program is developed to implement the formulation provided above. By using this program the influence of tooth modifications, introduced by: (a) the head-cutter blade profile consisting of two circular arcs (Fig. 1b), (b) the difference in head-cutter radii for the manufacture of the contacting tooth flanks of the pinion and the gear ($\Delta r_{t0}$), (c) the tilt and swivel angles of the cutter spindle with respect to the cradle rotation axis ($\kappa$ and $\mu$, Figs. 2 and 3), (d) the tilt distance ($h_d$, Fig. 3), (e) the variation in the radial machine

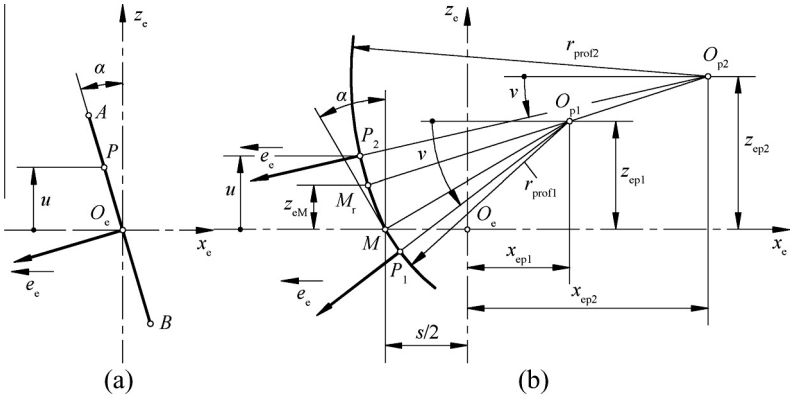


**Fig. 1** Head-cutter blade profiles.

tool setting ($e$, Figs. 2 and 3), and (f) the ratio of roll in the generation of pinion tooth-surfaces ($i_{g1}$), on load distribution, tooth contact pressure, transmission errors, and fillet stresses is investigated and discussed. Also, the correlation between the ease-off obtained by the modifications of pinion teeth and the tooth contact pressure distributions is investigated and the obtained results are presented.

## 2. Theoretical background

### 2.1. Definition of tooth surface geometry

In this study the concept of an imaginary generating crown gear is used to explain the generating cutting process of the face-hobbed spiral bevel pinion and gear teeth. This imaginary generating gear is a virtual gear whose teeth are formed by the traces of the cutting edges of the head-cutter blades, although its tooth number is not necessarily an integer. It can be considered as a special case of a bevel gear with 90 degree pitch angle. To obtain the pinion/gear tooth surface in the generating process, the work gear is rolled with the imaginary gear (Figs. 2 and 4).

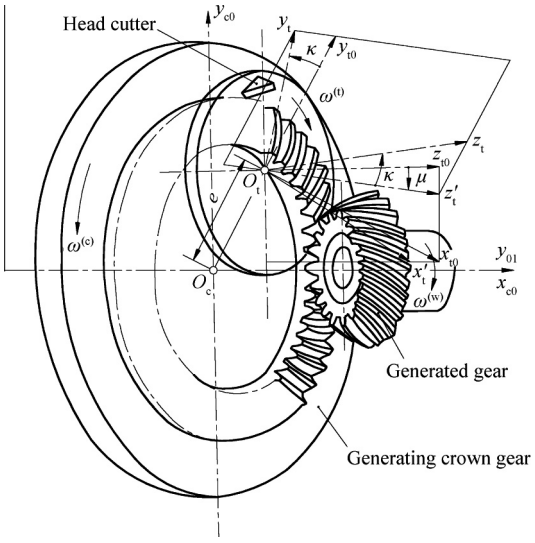


**Fig. 2** Concept of spiral bevel gear hobbing.

The tooth surface of the imaginary generating crown gear produced by coordinate transformation from coordinate system $K_e(x_e, y_e, z_e)$ (rigidly connected to the head-cutter) to coordinate system $K_c(x_c, y_c, z_c)$ (connected to the imaginary generating crown gear) is represented by the following matrix equation (based on Figs. 2 and 3):

$$\vec{r}_c = \boldsymbol{M}_{c4} \cdot \boldsymbol{M}_{c3} \cdot \boldsymbol{M}_{c2} \cdot \boldsymbol{M}_{c1} \cdot \vec{r}_e = \boldsymbol{M}_{ec} \cdot \vec{r}_e \tag{1}$$

where matrices $\boldsymbol{M}_{c1}$, $\boldsymbol{M}_{c2}$, $\boldsymbol{M}_{c3}$ and $\boldsymbol{M}_{c4}$ are presented in Ref. 41; $\vec{r}_e$ is the radius vector of the blade profile points (Fig. 1). The equation for $\vec{r}_e$ is presented in Ref. 41.

To obtain the tooth surface in the generating process, the work gears are rolled with the imaginary generating gear (Fig. 4). The concept of complementary imaginary generating crown gear is considered when the generated mating tooth surfaces of the pinion and the gear are fully conjugate. Conjugate means pinion and gear have a line contact in each angular position. The motion transmission happens in each roll position precisely with the same constant ratio. The contact area, the summation of all contact lines during the complete roll of one pair of teeth, is spread out over the entire active flank. To prevent stress concentrations on the tooth edges, caused by tooth errors, deflections under load, and misalignment between pinion and gear, a crowning in face width and in profile direction is applied to the pinion; the gear pair becomes "mismatched". In this case the generating crown gears for the pinion and the gear are not being complementarily identical.

Fig. 4 describes the coordinate systems between the imaginary generating crown gear and the work gears. The coordi-

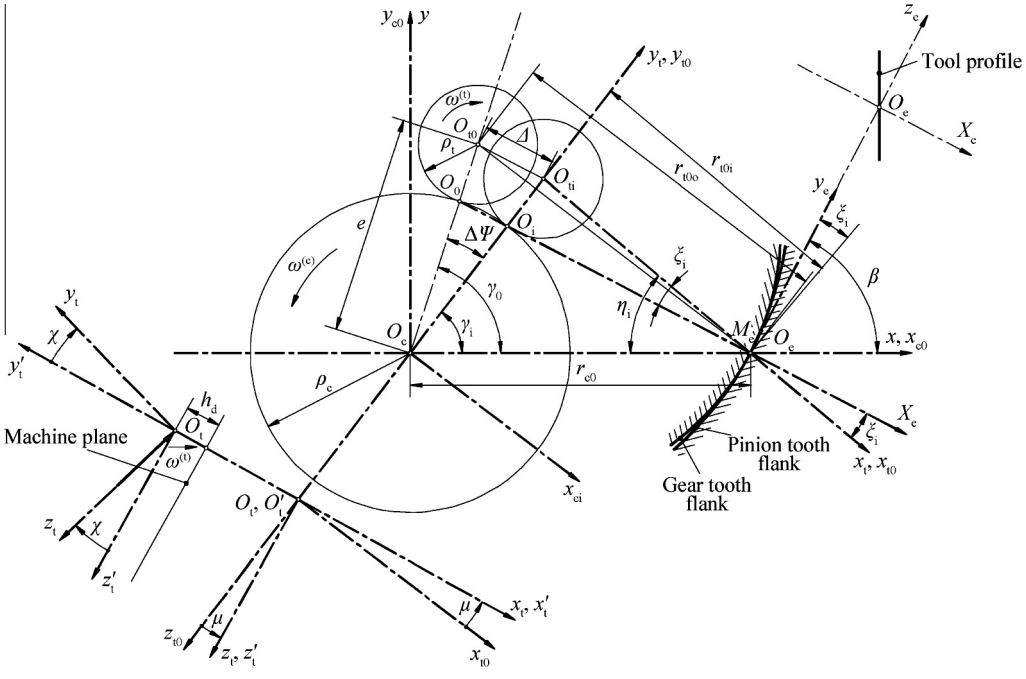


**Fig. 3** Relative position of head-cutter to imaginary generating crown gear.

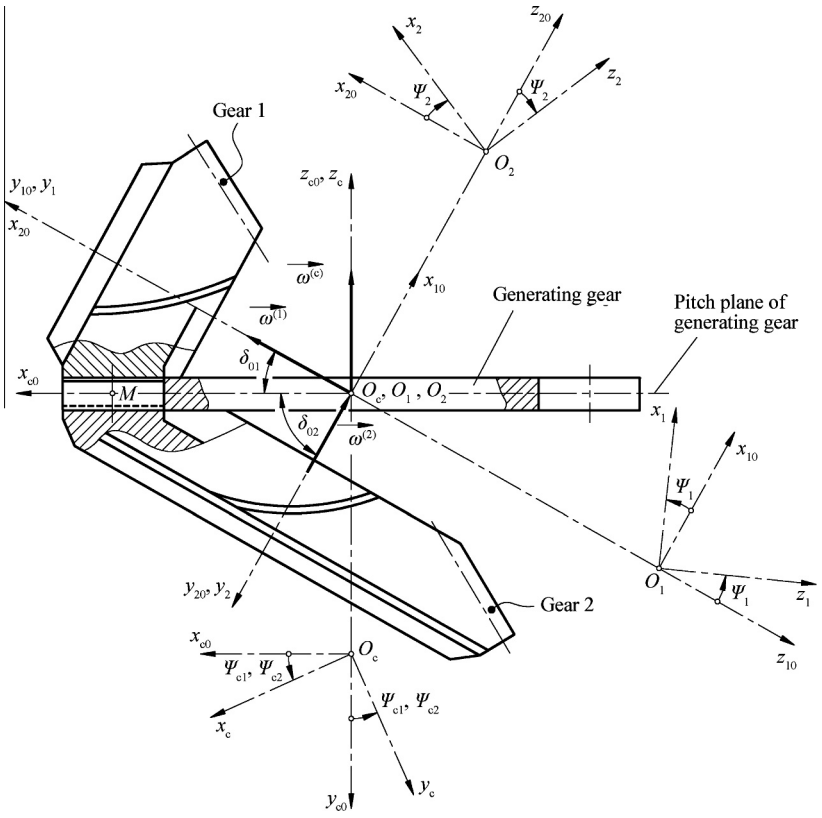


**Fig. 4** Generation of pinion and gear tooth-surfaces.

nate system $K_c(x_c, y_c, z_c)$ is rigidly connected to the generating crown gear; the coordinate systems $K_1(x_1, y_1, z_1)$ and $K_2(x_2, y_2, z_2)$ are rigidly connected to the pinion and the gear, respectively. The tooth surfaces of the pinion and of the gear are defined by the following system of equations:

$$\vec{r}_i^{(i)} = \boldsymbol{M}_{i3} \cdot \boldsymbol{M}_{i2} \cdot \boldsymbol{M}_{i1} \cdot \vec{r}_c^{(i)} = \boldsymbol{M}_{i3} \cdot \boldsymbol{M}_{i2} \cdot \boldsymbol{M}_{i1} \cdot \boldsymbol{M}_{ec} \cdot \vec{r}_e^{(i)} \tag{2a}$$

$$\vec{v}_{c0}^{(i,c)} \cdot \vec{e}_{c0}^{(i)} = 0 \tag{2b}$$

The coordinate transformations between the main coordinate systems $K_c(x_c, y_c, z_c)$, $K_1(x_1, y_1, z_1)$, $K_2(x_2, y_2, z_2)$, and the auxiliary coordinate systems (Fig. 4), are described in Ref. 41.

The fundamental equation of meshing (2b) states that, for each point to lie on the envelope tooth surface, the unit normal vector $\vec{e}_{c0}^{(i)}$ to the family of the generating crown gear surfaces should be perpendicular to the relative velocity of the generated pinion/gear to the generating crown gear, $\vec{v}_{c0}^{(i,c)}$.

### 2.2. Load distribution

The load distribution calculation is based on the conditions that the total angular position errors of the gear teeth being instantaneously in contact under load must be the same, and along the contact line (contact area) of every tooth pair instantaneously in contact, the composite displacements of tooth surface points – as the sums of tooth deformations, tooth surface separations, misalignments, and composite tooth errors – should correspond to the angular position of the gear member. Therefore, in all the points of the instantaneous contact lines the following displacement compatibility equation should be satisfied:

$$\Delta\Phi_2 = \Delta\Phi_2^{(d)} + \Delta\Phi_2^{(k)} = \frac{\Delta y_n}{r_D} \cdot \frac{|(\vec{r} \times \vec{a}_0) \cdot \vec{e}|}{|\vec{r}|} + \Delta\Phi_2^{(k)} \tag{3}$$

where $\Delta y_n$ is the composite displacement of contacting surfaces in the direction of the unit tooth surface normal $\vec{e}$, $\vec{r}$ is the position vector of the contact point, $r_D$ is the distance of the contact point to the gear axis, and $\vec{a}_0$ is the unit vector of the gear axis.

The composite displacement of the contacting surfaces in contact point $D$, in the direction of the tooth surface normal, can be expressed as

$$\Delta y_n = w(z_D) + s(z_D) + e_n(z_D) \tag{4}$$

where $z_D$ is the coordinate of point $D$ along the contact line, $w(z_D)$ the total deflection in point $D$, $s(z_D)$ the relative geometrical separation of tooth-surfaces in point $D$, and $e_n(z_D)$ the composite error in point $D$, that is the sum of manufacturing and alignment errors of pinion and gear.

The total deflection in point $D$ is defined by the following equation[31–33]

$$w(z_D) = \int_{L_{it}} K_d(z_D, z_F) \cdot p(z_F) \cdot \mathrm{d}z + K_c(z_D) \cdot p(z_D) \tag{5}$$

where $L_{it}$ is the geometrical length of the line of contact on tooth pair $i_t$, and $K_d(z_D, z_F)$ is the influence factor of tooth load acting in tooth-surface point $F$ on total composite deflection of pinion and gear teeth in contact point $D$. $K_d$ includes the bending and shearing deflections of pinion and gear teeth, pinion and gear body bending and torsion, and deflections of supporting shafts. A finite element computer program is developed for the calculation of bending and shearing deflections in the face-hobbed pinion and gear.[42] $K_c(z_D)$ is the influence factor for the

contact approach between contacting pinion and gear teeth, i.e., the composite contact deformation in point $D$ under load acting in the same point, $p(z_F)$ and $p(z_D)$ are the tooth loads acting in positions $F$ and $D$, respectively.

As the contact points are at different distances from the pinion/gear axis, the transmitted torque is defined by the equation

$$T = \sum_{i_t=1}^{i_t=N_t} \int_{L_{it}} r_F \cdot |\vec{\boldsymbol{p}}(z_F) \cdot \vec{\boldsymbol{t}}_{0F}| \cdot \mathrm{d}z \tag{6}$$

where $r_F$ is the distance of the loaded point $F$ to the gear axis, $\vec{\boldsymbol{t}}_{0F}$ is the tangent unit vector to the circle of radius $r_F$, passing through the loaded point $F$ in the transverse plane of the gear, and $N_t$ is the number of gear tooth pairs instantaneously in contact.

The load distribution on each line of contact can be calculated by solving the nonlinear system of Eqs. (3)–(6). An approximate and iterative technique is used to attain the solution. The contact lines are discretized into a suitable number of small segments, and the tooth contact pressure, acting along a segment, is approximated by a concentrated load, $\Delta\vec{\boldsymbol{F}}$, acting in the midpoint of the segment. By these approximations Eqs. (3), (4), and (6) become

$$\Delta\Phi_2 = \Delta y_{n(i_t,i_z)} \cdot \left( \frac{|(\vec{\boldsymbol{r}} \times \vec{\boldsymbol{a}}_0) \cdot \vec{\boldsymbol{e}}|}{r_D \cdot |\vec{\boldsymbol{r}}|} \right)_{(i_t,i_z)} + \Delta\Phi^{(k)}_{2(i_t)} \tag{7}$$

$$\Delta y_{n(i_t,i_z)} = w_{(i_t,i_z)} + s_{(i_t,i_z)} + e_{n(i_t,i_z)} \tag{8}$$

$$T = \sum_{i_t=1}^{i_t=N_t} \sum_{i_z=1}^{i_z=N_{z(i_t)}} r_{F(i_t,i_z)} \cdot |\Delta \vec{\boldsymbol{F}}_{(i_t,i_z)} \cdot \vec{\boldsymbol{t}}_{0F(i_t,i_z)}| \tag{9}$$

where $w_{(i_t,i_z)}$ is the total displacement in the midpoint of segment $i_z$ on tooth pair $i_t$, $\Delta\boldsymbol{F}_{(i_t,i_z)}$ the concentrated load acting in the midpoint of the segment, $i_t$ the identification number of contacting tooth pair, $i_z$ the segment identification number on tooth pair $i_t$, and $N_{z(i_t)}$ the number of segments on the contact line of tooth pair $i_t$ .

The total displacement is defined by the expression

$$w_{(i_t,i_z)} = w_{t(i_t,i_z)} + w_{c(i_t,i_z)} + w_{\mathrm{gs}(i_t,i_z)} \tag{10}$$

where $w_{t(i_t,i_z)}$ is the composite bending and shearing deflection of pinion and gear teeth, $w_{c(i_t,i_z)}$ the composite contact deformation of pinion and gear teeth, and $w_{\mathrm{gs}(i_t,i_z)}$ the deflection due to pinion and gear body bending and deflection of the supporting shafts.

The tooth deflections are obtained by the following summation

$$w_{t(i_t,i_z)} = \sum_{i_{z1}=1}^{i_{z1}=N_{z(i_t)}} \left( K^{(\mathrm{p})}_{d(i_t,i_{z1})} + K^{(\mathrm{g})}_{d(i_t,i_{z1})} \right) \cdot \Delta F_{(i_t,i_{z1})} \tag{11}$$

The compliances $K^{(\mathrm{p})}_{d(i_t,i_{z1})}$ and $K^{(\mathrm{g})}_{d(i_t,i_{z1})}$ for the pinion and the gear are defined by the following equation (based on Ref. 42):

$$\begin{aligned} K^{(\mathrm{p,g})}_{d(i_t,i_z)} = {} & \frac{c_{0\mathrm{w}}}{m \cdot E} \cdot N_1^{x_1} \cdot N_2^{x_2} \cdot \alpha^{x_3} \cdot \beta_0^{x_4} \cdot \left( \frac{b_{\mathrm{f}}}{m} \right)^{x_5} \cdot f_{\mathrm{k}}^{x_6} \cdot f_{\mathrm{f}}^{x_7} \\ & \cdot \left( \frac{s_{01}}{t_0} \right)^{x_8} \cdot \left( \frac{r_{\mathrm{fil}}}{m} \right)^{x_9} \cdot f_{\mathrm{wr0}}(h_{\mathrm{Fr}}, b_{\mathrm{Fr}}) \\ & \cdot f_{\mathrm{wa0}}(b_{\mathrm{Fr}}, h_{\mathrm{Fr}}) \cdot f_{\mathrm{wr}}(h_{Dr}, h_{Fr}) \\ & \cdot f_{\mathrm{wa}}(b_{Dr}, h_{Fr}) \quad (\mathrm{mm/N}) \end{aligned} \tag{12}$$

The actual load distribution, defined by the values of loads $\Delta\vec{\boldsymbol{F}}$, is obtained by using the successive-over-relaxation method. In every iteration cycle a search for the points of the "potential" contact lines that could be in instantaneous contact is performed. For these points the following condition should be satisfied

$$\Delta y_{n(i_t,i_z)} \leqslant \frac{\Delta\Phi_2 - \Delta\Phi^{(\mathrm{k})}_{2(i_t)}}{\left( \dfrac{|(\vec{\boldsymbol{r}} \times \vec{\boldsymbol{a}}_0) \cdot \vec{\boldsymbol{e}}|}{r_D \cdot |\vec{\boldsymbol{r}}|} \right)_{(i_t,i_z)}} \tag{13}$$

The details of the method for load distribution calculation in face-milled spiral bevel gears are described in Ref. 32.

### 2.3. Maximum fillet stresses

The maximum fillet stress belonging to the normal section $i_z$ on tooth $i_t$ is determined by the following summation:

$$\sigma_{\mathrm{fil\,max}(i_t,i_z)} = \sum_{i_{z1}=1}^{i_{z1}=N_{z(i_t)}} K_{\sigma(i_t,i_{z1})} \cdot \Delta F_{(i_t,i_{z1})} \tag{14}$$

where (based on Ref. 42)

$$\begin{aligned} K_{\sigma(i_t,i_z)} = {} & \frac{c_\sigma}{m^2} \cdot N_1^{y_1} \cdot N_2^{y_2} \cdot \alpha^{y_3} \cdot \beta_0^{y_4} \cdot \left( \frac{b_{\mathrm{f}}}{m} \right)^{y_5} \cdot f_{\mathrm{k}}^{y_6} \cdot f_{\mathrm{f}}^{y_7} \cdot \left( \frac{s_{01}}{t_0} \right)^{y_8} \\ & \cdot \left( \frac{r_{\mathrm{fil}}}{m} \right)^{y_9} \cdot f_{\sigma\mathrm{r0}}(h_{\mathrm{Fr}}, b_{\mathrm{Fr}}) \\ & \cdot f_{\sigma\mathrm{a0}}(b_{\mathrm{Fr}}, h_{\mathrm{Fr}}) \cdot f_{\sigma\mathrm{a}}(b_{\mathrm{Dr}}, h_{\mathrm{Fr}}) \quad (\mathrm{mm}^{-2}) \end{aligned} \tag{15}$$

### 2.4. Transmission errors

The total transmission error consists of the kinematical transmission error due to the mismatch of the gear pair and due to eventual tooth errors and misalignments of the meshing members, and of the transmission error caused by the deflection of teeth (Eq. (3)).

It is assumed that the pinion is the driving member that is rotating at a constant velocity. As the result of the mismatch of gears, a changing angular velocity ratio of the gear pair and an angular displacement of the driven gear member from the theoretically exact position based on the ratio of the numbers of teeth occur. This angular displacement of the gear can be expressed as

$$\Delta\Phi^{(\mathrm{k})}_2 = \Phi_2 - \Phi_{20} - N_1 \cdot (\Phi_1 - \Phi_{10})/N_2 + \Delta\Phi_{2s} \tag{16}$$

where $\Phi_{10}$ and $\Phi_{20}$ are the initial angular positions of the pinion and the gear, $\Phi_2$ is the instantaneous angular position of the gear for a particular angular position of the pinion, $\Phi_1$; $N_1$ and $N_2$ are the numbers of pinion and gear teeth, respectively; and $\Delta\Phi_{2s}$ is the angular displacement of the gear due to edge contact in the case of misalignments of the mating members when a "negative" separation occurs on a tooth pair different from the tooth pair for which the angular position is calculated.

The angular displacement of the gear, $\Delta\Phi^{(\mathrm{d})}_2$, caused by the variation of the compliance of contacting pinion and gear teeth rolling through mesh, is determined in the load distribution calculation(Eq. (3)).

Therefore, the total angular position error of the gear is defined by the equation

$$\Delta\Phi_2 = \Delta\Phi^{(\mathrm{k})}_2 + \Delta\Phi^{(\mathrm{d})}_2 \tag{17}$$

**Table 1** Pinion and gear design data.

| Parameter | Pinion | Gear |
|---|---|---|
| Number of teeth | 12 | 36 |
| Module (mm) | 4.941 | |
| Pressure angle (°) | 20 | |
| Mean spiral angle (°) | 35 | |
| Face width (mm) | 25.4 | |
| Pitch diameter (mm) | 59.292 | 177.876 |
| Outside diameter (mm) | 65.931 | 178.761 |
| Pitch angle (°) | 18.4349 | 71.5651 |

## 3. Results

A computer program was developed to implement the formulation provided above. By using this program the influence of modifications, introduced by: the radii of the head-cutter profile ($r_{prof1}$ and $r_{prof2}$), the difference in head-cutter radii for the manufacture of the contacting tooth flanks of the pinion and the gear ($\Delta r_{t0}$), the variation in the radial machine tool setting ($e$), the variation in the ratio of roll in the generation of pinion tooth-surfaces ($i_{g1}$), the tilt distance ($h_d$), the tilt and swivel angles of the cutter spindle with respect to the cradle rotation axis ($\kappa$ and $\mu$), and by the combination of variations in different machine tool settings, on tooth flank form, load distribution, tooth contact pressure, transmission errors, and fillet stresses is investigated. The main design data of the example spiral bevel gear pair used in this study is given in Table 1.

The load distribution calculations were performed for 21 instantaneous positions of the mating members rolling through a mesh cycle. Part of the obtained results is presented in Fig. 5. In these figures factors $k_{p\max}$, $k_{\beta F\max}$, $k_{\Delta\phi 2\max}$, $k_{\sigma fil}$ represent the ratios of the maximum values of tooth contact pressure ($p_{max}$), load distribution factor ($\beta_{Fmax}$), angular displacement of the driven gear member ($\Delta\Phi_{2max}$), and maximum fillet stresses ($\sigma_{filmax}$) in the pinion and the gear obtained by applying arbitrarily chosen values of profile radii and machine-tool settings, and the values of $p_{max0}$, $\beta_{Fmax0}$, $\Delta\Phi_{2max0}$, and $\sigma_{filmax0}$ obtained by applying straight-lined head-cutter profile and the basic machine-tool setting ensuring the full conjugation of meshing tooth surfaces. It means that $k_{p\max} = \frac{p_{max}}{p_{max0}}$, $k_{\beta F\max} = \frac{\beta_{F\max}}{\beta_{F\max 0}}$, $k_{\Delta\Phi_{2\max}} = \frac{\Delta\Phi_{2max}}{\Delta\Phi_{2max0}}$, and $k_{\sigma fil} = \frac{\sigma_{fil\,max}}{\sigma_{fil\,max\,0}}$. For the gear pair with truly conjugate tooth surfaces rolling through a mesh cycle it was obtained: $p_{max0} = 1155$ MPa, $\beta_{Fmax0} = 1.9496$, and $\Delta\Phi_{2max0} = 12.23$ arcsec. It can be observed in Fig. 5 that the use of a head-cutter with circular profile and the variation in machine tool settings have an extremely strong effect on the angular displacement of the driven gear member and in some cases on fillet stresses. Solutions to reduce the maximum tooth contact pressure and/or the maximum transmission error are shown in Table 2. The maximum tooth contact pressure reduction can be achieved by applying a combination of the tilt and swivel angles of $\kappa = 2°$, $\mu = -1°$, the variation in radial machine tool setting of $\Delta e = -0.01$ mm and the variation in the ratio of roll in the generation of pinion tooth-surfaces of $\Delta i_{g1} = 0.002$. In this case, the maximum tooth contact pressure is reduced to $p_{max} = 424$ MPa, but the transmission error increases to $\Delta\Phi_{2max} = 13.80$ arcsec. The maximum angular position error of the driven gear can be reduced to $\Delta\Phi_{2max} = 2.18$ arcsec by applying tilt and swivel angles of $\kappa = 2°$, $\mu = -1°$, respectively, in combination with the tilt distance of $h_d = 0.15$ mm. In this case, the maximum tooth contact pressure is moderately reduced to $p_{max} = 671$ MPa. A balanced reduction of the maximum tooth contact pressure and the transmission error is obtained by applying a head cutter whose profile consists of a straight-lined segment and a circular arc of radius $r_{prof1} = 580$ mm, combined with a difference in the head-cutter radii for the manufacture of the contacting tooth flanks of the pinion and the gear of $\Delta r_{t0} = 0.7$ mm: $p_{max} = 535$ MPa and $\Delta\Phi_{2max} = 4.67$ arcsec.

To validate the obtained results for face-hobbed spiral bevel gear pairs with different design data, the influence of the gear ratio on tooth contact pressure and transmission error is investigated. The gear ratio is changed by the variation in

**Table 2** Reductions of maximum tooth contact pressure and transmission errors.

| Parameter | $p_{max}$ (MPa) | $\Delta\varphi_{2max}$ (arcsec) |
|---|---|---|
| Truly conjugate tooth surfaces | 1155 | 12.23 |
| $r_{prof1} = 100$ mm, $r_{prof2} = 0$ | 622 | 24.17 |
| $r_{prof1} = 250$ mm, $r_{prof2} = 0$ | 592 | 14.77 |
| $r_{prof1} = 1000$ mm, $r_{prof2} = 0$ | 902 | 8.72 |
| $r_{prof1} = 0$, $r_{prof2} = 1000$ mm | 1164 | 9.38 |
| $r_{prof1} = r_{prof2} = 250$ mm | 604 | 15.85 |
| $r_{prof1} = r_{prof2} = 1000$ mm | 913 | 9.38 |
| $\Delta r_{t0} = 0.279$ mm | 789 | 6.88 |
| $\Delta r_{t0} = 0.559$ mm | 704 | 8.62 |
| $\Delta e = -0.05$ mm | 467 | 25.26 |
| $\Delta e = 0.01$ mm | 1283 | 7.95 |
| $\Delta i_{g1} = 0.003$ | 445 | 27.33 |
| $h_d = 1$ mm | 1091 | 7.84 |
| $\kappa = 2°$, $\mu = -1°$ | 663 | 2.43 |
| $\kappa = 2°$, $\mu = -1°$, $\Delta e = -0.02$ mm | 548 | 5.22 |
| $\kappa = 2°$, $\mu = -1°$, $\Delta e = -0.01$ mm, $\Delta i_{g1} = 0.003$ | 429 | 13.80 |
| $\kappa = 2°$, $\mu = -1°$, $h_d = 0.15$ mm | 671 | 2.18 |
| $\kappa = 2°$, $\mu = -1°$, $\Delta i_{g1} = 0.003$, $h_d = 3$ mm | 595 | 5.54 |
| $\Delta r_{t0} = 0.7$ mm, $r_{prof1} = 580$ mm | 535 | 4.67 |

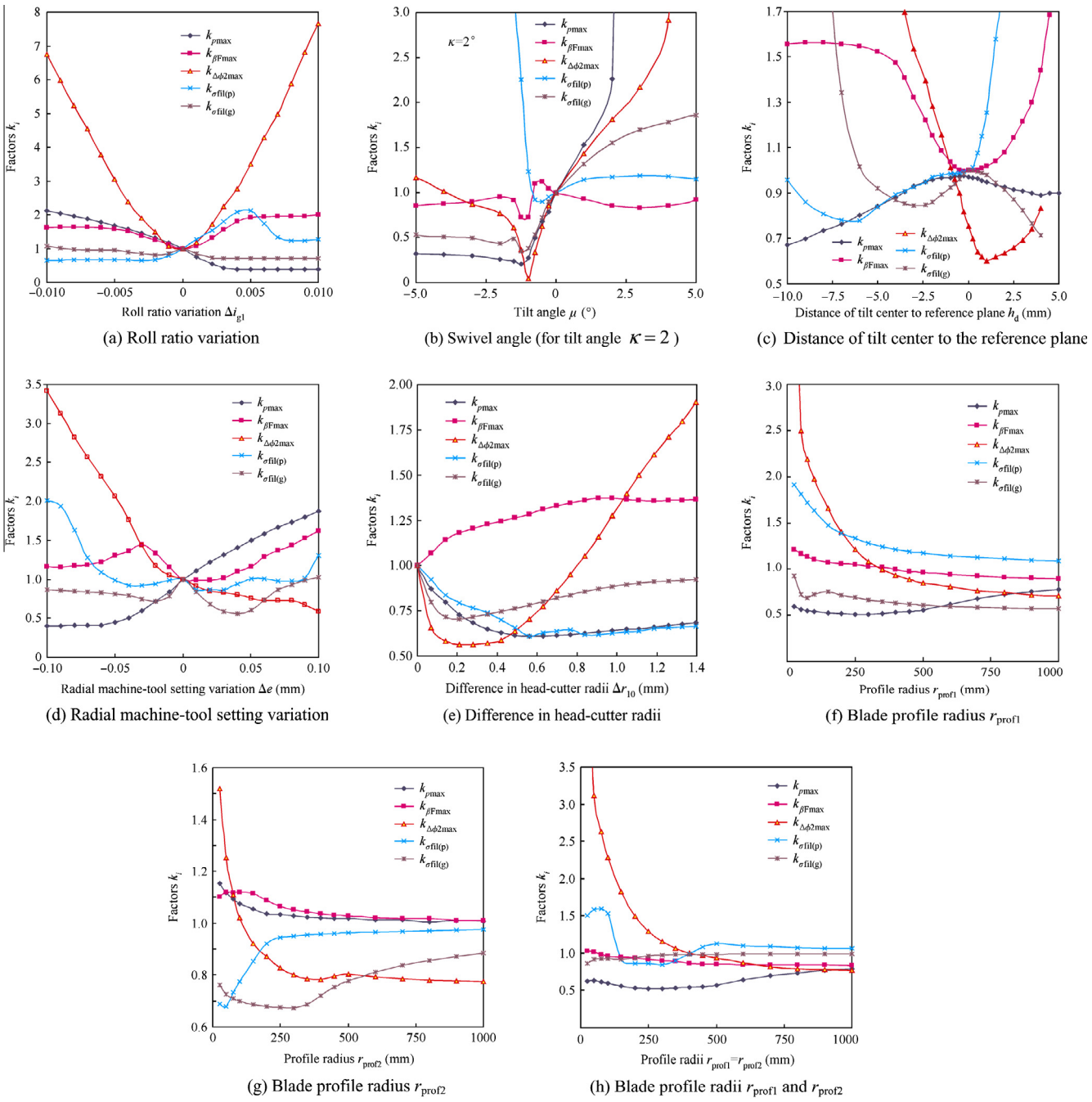


**Fig. 5** Influence of $\Delta i_{g1}$, $\mu$, $h_d$, $\Delta e$, $\Delta r_{t0}$, $r_{prof1}$ and $r_{prof2}$ on $p_{max}$, $\beta_{Fmax}$, $\Delta\varphi_{2max}$, and $\sigma_{filmax(p)}$, $\sigma_{filmax(g)}$.

the numbers of teeth of the pinion and the gear. The obtained results are shown in Figs. 6–8. In Fig. 6, it can be observed that for all gear tooth numbers, the combination of the profile radius of $r_{prof1}$ = 580 mm and of the difference in the head-cutter radii for the manufacture of the contacting tooth flanks of the pinion and the gear of $\Delta r_{t0}$ = 0.7 mm reduces simultaneously the maximum tooth contact pressure and the transmission error. The other combinations of machine tool setting variations reduce the tooth contact pressure, but increase the transmission errors for almost all gear tooth numbers. By applying the combination of a head-cutter with profile radius of $r_{prof1}$ = 580 mm and difference in the head-cutter radii for the manufacture of the contacting tooth flanks of the pinion and the gear of $\Delta r_{t0}$ = 0.7 mm, both the tooth contact pressure and the transmission errors are reduced for pinion tooth numbers of 9 and 15, too (Figs. 7 and 8).

The ease-off and tooth contact pattern regarding tooth flank modifications introduced by curvilinear head-cutter profile, head-cutter diameter difference, and machine tool setting variations are shown in Figs. 9–20. In the present paper, the term ease-off indicates modifications of the tooth flank form with respect to its basic design. The modifications are introduced only in the pinion teeth; therefore, the ease-off is achieved by the topology of the pinion tooth. The ease-off dia-

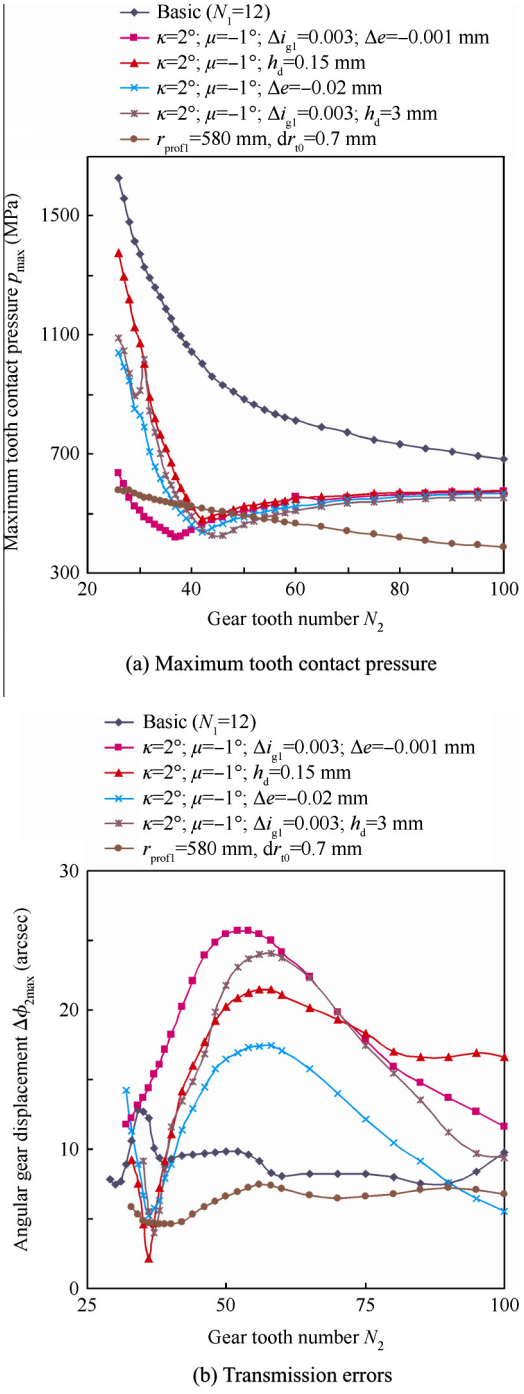


**Fig. 6** Influence of gear tooth number, head-cutter profile and diameter, and machine tool settings on maximum tooth contact pressure and transmission errors.

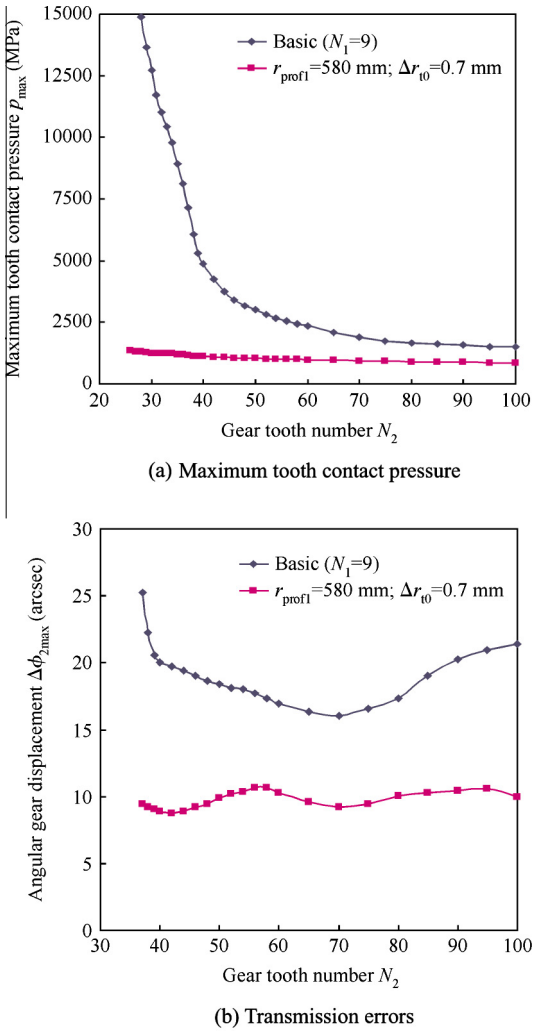


**Fig. 7** Influence of gear tooth number and head-cutter profile and diameter on maximum tooth contact pressure and transmission errors in the case of pinion tooth number $N_1 = 9$.

grams in Figs. 9–20 represent the amounts of removed material inside the theoretical (nomodified) pinion tooth surface related to grid points. Therefore, the ease-off increases the geometrical separation of contacting tooth surfaces. In Figs. 9–20 the tooth contact pressure distributions are plotted on the gear tooth flank, and the ease-off is represented on the pinion-based two-dimensional domain, obtained by mapping the pinion's three-dimensional tooth points $(x_1, y_1, z_1)$ to the axial plane coordinates $(r_1, y_1)$ of the pinion, where $r = \sqrt{x_1^2 + z_1^2}$ .

The tooth contact pressure distributions along the potential contact lines for 21 instantaneous positions of the mating members rolling through a mesh cycle and for all the adjacent tooth pairs engaged for a particular position of the mating members, for the case when no modifications are introduced into the pinion teeth, are shown in Fig. 9. In this case the pinion and gear tooth surfaces are fully conjugate and no ease-off exists. It can be observed that there is an unbalanced pressure distribution with pressure peaks along the edge on the tooth heel. The use of a head-cutter with circular arc profiles causes ease-off in the tooth height direction, with mixed results in the reduction of the maximum tooth contact pressure and transmission errors (Fig. 10). The difference in head-cutter radii for the manufacture of the contacting tooth flanks of the pinion and the gear of $\Delta r_{t0} = 0.56$ mm results in a considerable ease-off in the tooth length direction composed with a slight twisting, and moderate reductions in the maximum tooth con-

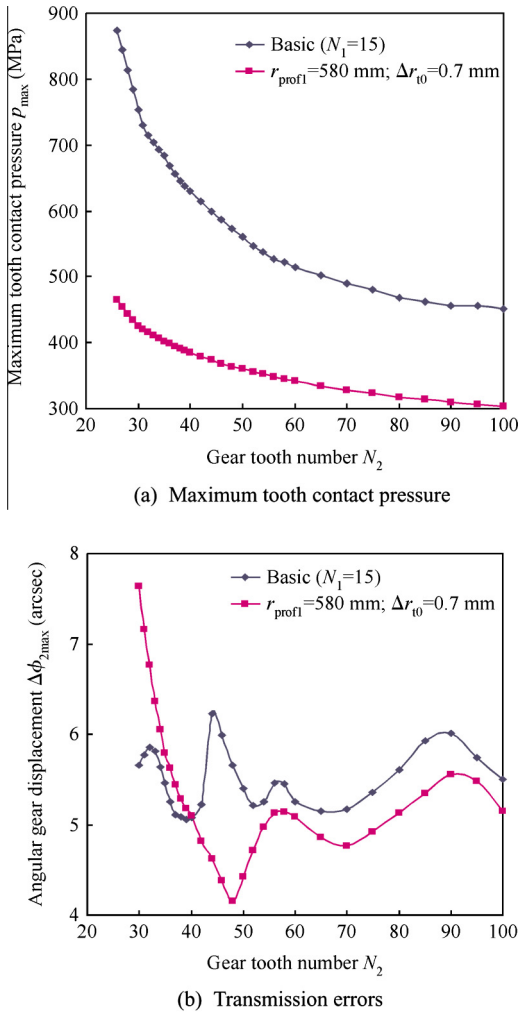


**Fig. 8** Influence of gear tooth number and head-cutter profile and diameter on maximum tooth contact pressure and transmission errors in the case of pinion tooth number $N_1 = 15$.

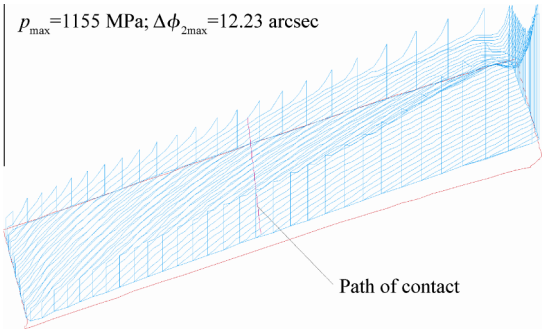


**Fig. 9** Tooth contact pressure distributions along contact lines of conjugate tooth surfaces for all tooth pairs in instantaneous contact for 21 positions of meshing members through a mesh cycle.

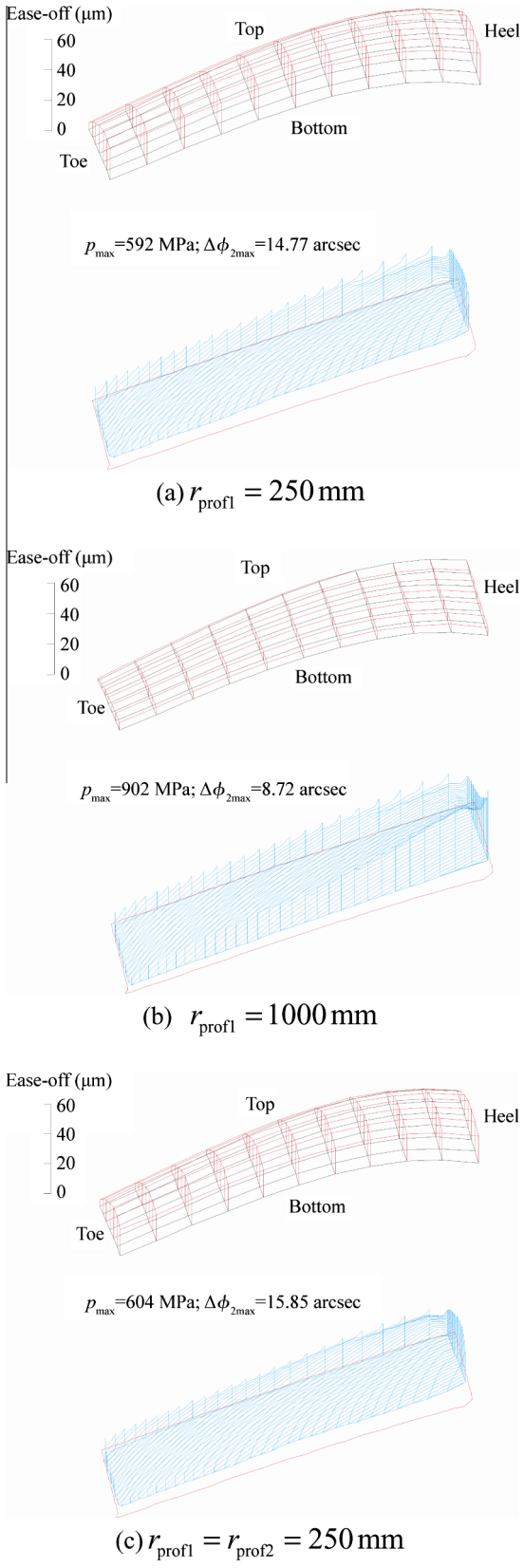


**Fig. 10** Ease-off and tooth contact pressure distributions for blade profile.

tact pressure and transmission error (Fig. 11). By the variation in the radial machine tool setting of $\Delta e = -0.05$ mm ease-off on the tooth heel is obtained (Fig. 12), with a big reduction in the maximum tooth contact pressure, but accompanied with

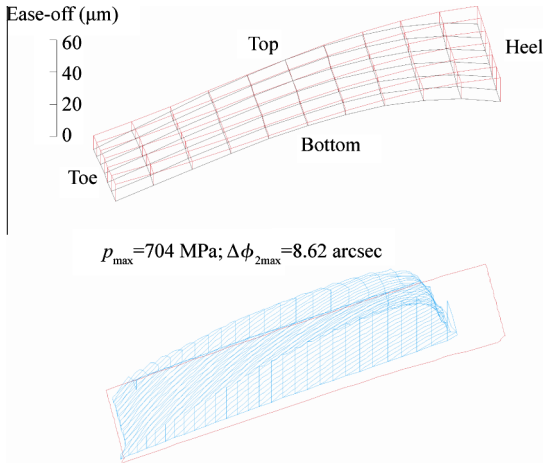


**Fig. 11** Ease-off and tooth contact pressure distributions in the case of the difference in head-cutter radii for the manufacture of contacting tooth flanks of the pinion and the gear $\Delta r_{t0} = 0.56$ mm.

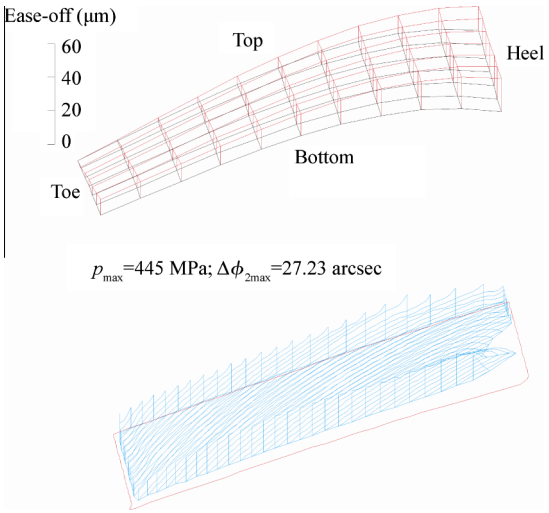


**Fig. 13** Ease-off and tooth contact pressure distributions for the variation in the ratio of roll in the generation of pinion tooth-surfaces of $\Delta i_{g1} = 0.003$.

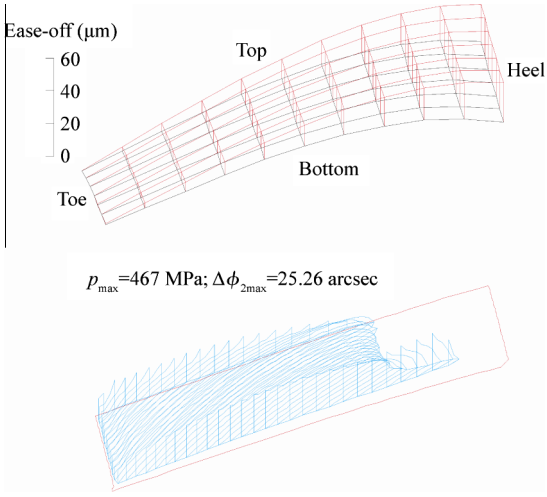


**Fig. 12** Ease-off and tooth contact pressure distributions for radial machine tool setting variation $\Delta e = -0.05$ mm.

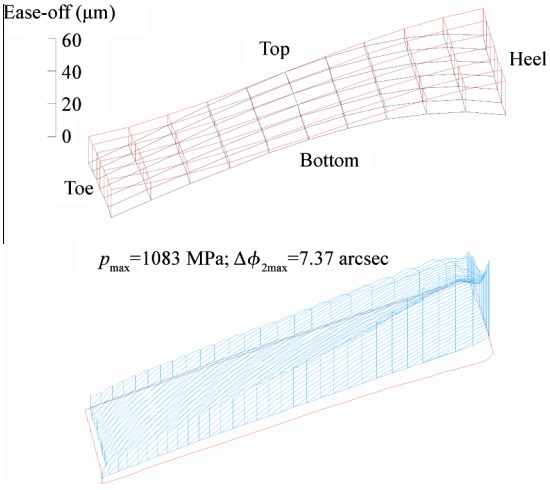


**Fig. 14** Ease-off and tooth contact pressure distributions for distance of tilt center to the reference plane of $h_d = 1$ mm.

a big increase in the angular displacement of the driven gear. The tooth contact pattern does not cover the whole tooth surface. A twisted ease-off, a much uniform pressure distribution, and a bigger tooth contact pattern are obtained by the variation in the ratio of roll for the generation of pinion tooth-surfaces of $\Delta i_{g1} = 0.003$ (Fig. 13). The maximum tooth pressure is reduced to $p_{max} = 445$ MPa, but a considerable increase in the maximum transmission error to $\Delta\Phi_{2max} = 27.33$ arcsec occurs. The maximum ease-off values are on the toe and on the heel of the tooth by applying a distance of the tilt center to the reference plane of $h_d = 1$ mm (Fig. 14), but no considerable reduction in the maximum tooth contact pressure is obtained. A big reduction in transmission error to $\Delta\Phi_{2max} = 2.47$ arcsec can be achieved by applying a combination of the tilt and swivel angles of $\kappa = 2°$, $\mu = -1°$, respectively (Fig. 15). The corresponding tooth modifications also result in a considerable reduction in the maximum tooth contact pressure to $p_{max} = 661$ MPa.

Much bigger and/or balanced reduction of the maximum tooth contact pressure and transmission errors can be achieved by the combination of optimal head-cutter profile, difference in head-cutter radii for the manufacture of the contacting tooth flanks of the pinion and the gear, and machine tool settings. A twisted ease-off and a balanced reduction of maximum tooth contact pressure and transmission error is obtained by the combination of the tilt and swivel angles and the variation in the radial machine tool setting of: $\kappa = 2°$, $\mu = -1°$, and $\Delta e = -0.02$ mm (Fig. 16). By combining the above amounts of tilt and swivel angles with the variation in the radial machine tool setting of $\Delta e = -0.01$ mm

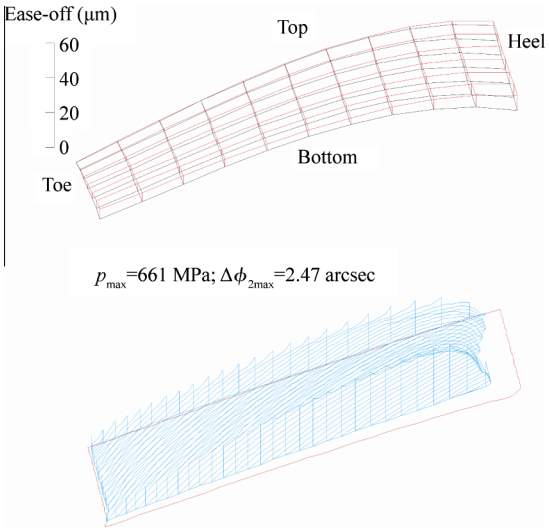


**Fig. 15** Ease-off and tooth contact pressure distributions for the combination of tilt angle $\kappa = 2°$ and swivel angle $\mu = -1°$.

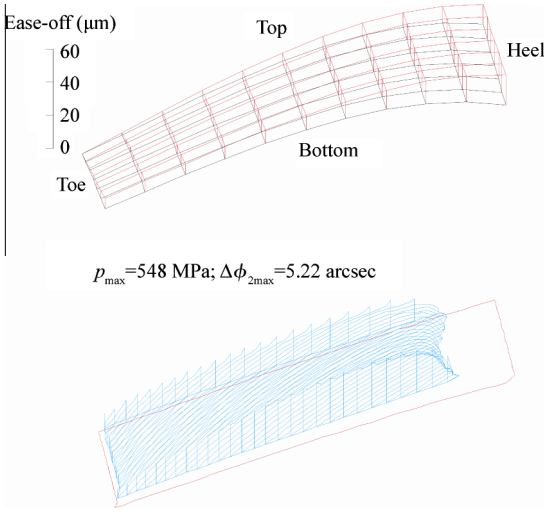


**Fig. 16** Ease-off and tooth contact pressure distributions for the combination of tilt angle $\kappa = 2°$, swivel angle $\mu = -1°$, and radial machine tool setting variation $\Delta e = -0.02$ mm.

and in the ratio of roll for the generation of pinion tooth-surfaces of $\Delta i_{g1} = 0.003$, a much bigger ease-off on the tooth heel is obtained; the maximum tooth contact pressure is reduced to $p_{max} = 429$ MPa, but the transmission error slightly increases to $\Delta\Phi_{2max} = 13.80$ arcsec (Fig. 17). The same numbers of the tilt and swivel angles in combination with the distance of the tilt center to the reference plane of $h_d = 1$ mm result in a relatively small ease-off, maximum reduction of transmission error to $\Delta\Phi_{2max} = 2.18$ arcsec, and a considerable reduction of maximum tooth contact pressure to $p_{max} = 671$ MPa (Fig. 18). The combination of $\kappa = 2°$, $\mu = -1°$,

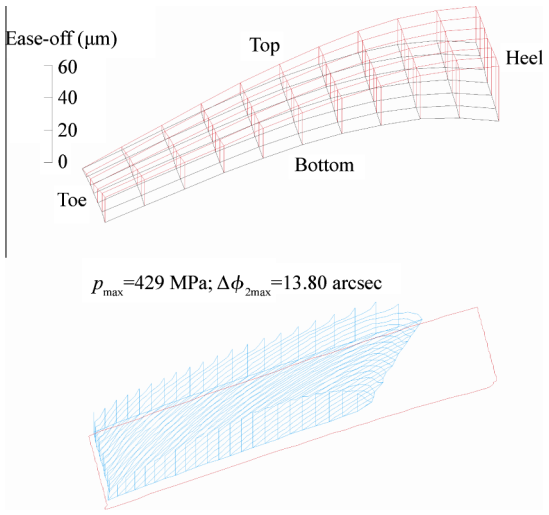


**Fig. 17** Ease-off and tooth contact pressure distributions for the combination of tilt angle $\kappa = 2°$, swivel angle $\mu = -1°$, radial machine tool setting variation $\Delta e = -0.01$ mm, and the variation in the ratio of roll in the generation of pinion tooth-surfaces of $\Delta i_{g1} = 0.003$.

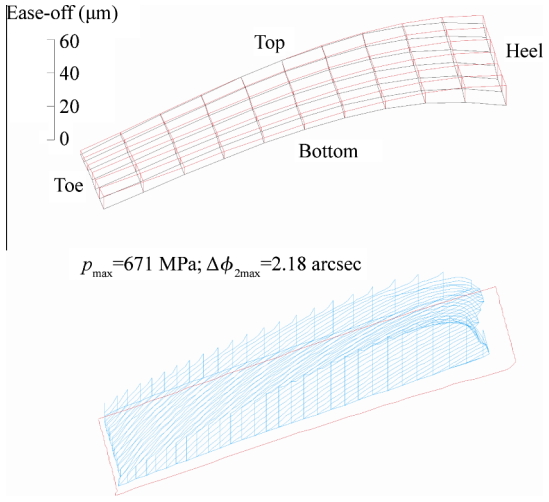


**Fig. 18** Ease-off and tooth contact pressure distributions for the combination of tilt angle $\kappa = 2°$, swivel angle $\mu = -1°$, and distance of tilt center to the reference plane of $h_d = 0.15$ mm.

$\Delta i_{g1} = 0.003$, and $h_d = 3$ mm causes big ease-offs on the toe and on the heel of teeth and a balanced reduction of the maximum tooth contact pressure and transmission error (Fig. 19). A much moderate ease-off and balanced maximum tooth contact pressure and transmission error reductions are the results of the combination of head-cutter profile radius of $r_{profl} = 580$ mm and of the difference in head-cutter radii for the manufacture of the contacting tooth flanks of the pinion and the gear of $\Delta r_{t0} = 0.7$ mm (Fig. 20).

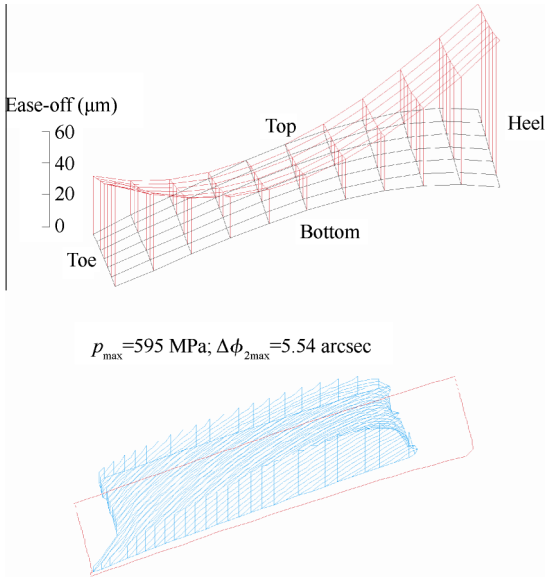


**Fig. 19** Ease-off and tooth contact pressure distributions for the combination of tilt angle $\kappa = 2°$, swivel angle $\mu = -1°$, the variation in the ratio of roll in the generation of pinion tooth-surfaces of $\Delta i_{g1} = 0.003$, and distance of tilt center to the reference plane of $h_d = 3$ mm.

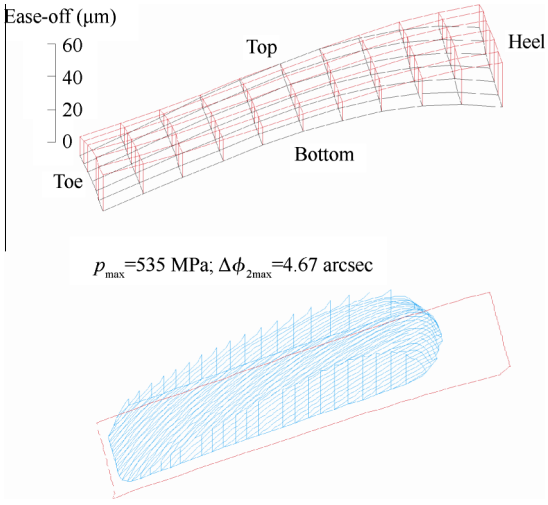


**Fig. 20** Ease-off and tooth contact pressure distributions for blade profile radius $r_{prof1} = 580$ mm and difference in head-cutter radii for the manufacture of the contacting tooth flanks of the pinion and the gear $\Delta r_{t0} = 0.7$ mm.

## 4. Conclusions

The influence of modifications introduced into the pinion tooth-surface by applying curvilinear head-cutter profile and machine-tool setting variations, on load distribution, maximum tooth contact pressure, transmission errors, and fillet stresses is investigated. On the basis of the obtained results, for the investigated face-hobbed spiral bevel gear example, the following conclusions can be drawn:

(1) The biggest and balanced reduction of maximum tooth contact pressure and transmission error can be achieved by the combination of optimal head-cutter profile, difference in head-cutter radii for the manufacture of the contacting tooth flanks of the pinion and the gear, and machine tool settings.

(2) Extremely big reduction in the maximum tooth contact pressure is obtained ($p_{max} = 424$ MPa) by applying a combination of tilt and swivel angles of $\kappa = 2°$, $\mu = -1°$, with variations in the radial machine tool setting of $\Delta e = -0.01$ mm and ratio of roll in the generation of pinion tooth-surfaces of $\Delta i_{g1} = 0.002$. The transmission error slightly increases to $\Delta\varphi_{2max} = 13.80$ arcsec.

(3) The same numbers of the tilt and swivel angles as above, in combination with the distance of the tilt center to the reference plane of $h_d = 1$ mm result in the maximum reduction of transmission error to $\Delta\varphi_{2max} = 2.18$ arcsec, and a considerable reduction of the maximum tooth contact pressure to $p_{max} = 671$ MPa.

(4) A balanced, considerable big reduction of the maximum tooth contact pressure and of the transmission error is obtained by applying a head cutter whose profile consists of a straight-lined segment and a circular arc of radius $r_{prof1} = 580$ mm, combined with a difference in the head-cutter radii for the manufacture of the contacting tooth flanks of the pinion and the gear $\Delta r_{t0} = 0.7$ mm: $p_{max} = 535$ MPa and $\Delta\varphi_{2max} = 4.67$ arcsec. It is the optimal solution.

## Acknowledgement

The author would like to thank the Hungarian Scientific Research Fund (OTKA) for their financial support of the research under Contract No. K77921.

## References

1. Litvin FL. *Theory of gear mesh*. Budapest: Műszaki Könyvkiadó; 1972 [Hungarian].
2. Litvin FL, Chang WS, Lundy M, Tsung WJ. Design of pitch cones for face-hobbed hypoid gears. *ASME J Mech Des* 1990;**112**:413–8.
3. Kawasaki K, Tamura H, Nakano Y. A method for inspection of spiral bevel gears in Klingelnberg cyclo-palloid system. In: *Proceedings of the international gearing conference*, Newcastle upon Tyne; 1994. p. 305–10.
4. Kawasaki K, Tamura H, Iwamoto Y. Klingelnberg spiral bevel gears with small spiral angles. In: *Proceedings of the 4th world congress on gearing and power transmissions*, Paris; 1999. p. 697–703.
5. Kawasaki K. Manufacturing Method for large-sized bevel gears in cylo-palloid system using multi-axis control and multi-tasking machine tool. In: *Proceedings of international conference on gears*, Munich: VDI-Berichte 2108.1; 2010. p. 337–48.
6. Kato S, Kubo A. Analysis of the effect of cutting dimensions on the performance of hypoid gears manufactured by the hobbing process. In: *Proceedings of 4th world congress on gearing and power transmissions*, Paris; 1999. p. 585–94.
7. Kato S, Ikebe H, Hiramatsu J. Study on the tooth surface modification of hypoid gear in face hob system. In: *Proceedings of JSME international conference on motion and power transmissions*, Sendai; 2009. p. 109–11.

8. Stadtfeld HJ. *The basics of gleason face hobbing*. Gleason Works; 2000, p. 1–26.
9. Lelkes M, Márialigeti J, Play D. Numerical determination of cutting parameters for the control of Klingelnberg spiral bevel gear geometry. *ASME J Mech Des* 2002;**124**:761–71.
10. Fan Q. Computerized modeling and simulation of spiral bevel and hypoid gears manufactured by gleason face hobbing process. *ASME J Mech Des* 2006;**128**:1315–27.
11. Fan Q. Enhanced algorithms of contact simulation for hypoid gear drives produced by face-milling and face-hobbing processes. *ASME J Mech Des* 2007;**129**:31–7.
12. Fan Q. Tooth surface error corrections for face-hobbed hypoid gears. *ASME J Mech Des* 2010;**132**:011004-1-8.
13. Shih YP, Fong ZH, Lin DCY. Mathematical model for a universal face hobbing hypoid gear generator. *ASME J Mech Des* 2007;**129**:38–47.
14. Shih YP, Fong ZH. Flank modification methodology for face-hobbing hypoid gears based on ease-off topology. *ASME J Mech Des* 2007;**129**:1294–302.
15. Shih YP. A novel ease-off flank modification methodology for spiral bevel and hypoid gears. *Mech Mach Theory* 2010;**45**: 1108–24.
16. Vimercati M. Mathematical model for tooth surfaces representation of face-hobbed hypoid gears and its application to contact analysis and stress calculation. *Mech Mach Theory* 2007;**42**:668–90.
17. Zhang Y, Wu Z. Geometry of tooth profile and fillet of face-hobbed spiral bevel gears. In: *Proceedings of the 10th ASME international power transmission and gearing conference*, Las Vegas: Paper No. DETC2007/PTG-34123; 2007. p. 1–12.
18. Wilcox LE. An exact analytical method for calculating stresses in bevel and hypoid gear teeth. In: *Proceedings of international symposium on gearing and power transmissions*, Tokyo, II; 1981. p. 115–21.
19. Bibel GD, Kumar A, Reddy S, Handschuh RF. Contact stress analysis of spiral bevel gears using finite element analysis. *ASME J Mech Des* 1995;**117**:235–40.
20. Gosselin C, Cloutier L, Nguyen QD. A general gormulation for the calculation of the load sharing and transmission error under load of spiral bevel and hypoid gears. *Mech Mach Theory* 1995;**30**:433–50.
21. Handschuh RF, Bibel GD. Experimental and analytical study of aerospace spiral bevel gear tooth fillet stresses. *ASME J Mech Des* 1999;**121**:565–72.
22. Fang Z, Yang H. Loaded tooth contact analysis with friction on hypoid gears. In: *Proceedings of 4th world congress on gearing and power transmissions*, Paris; 1999. p. 703–10.
23. Linke H, Haase A, Hnecke C, Hutschenreiter B, Trempler U. A new methodology for the calculation of the geometry, the contact pattern and the gear load capacity of bevel gears. In: *Proceedings of 4th world congress on gearing and power transmissions*, Paris; 1999. p. 623–34.
24. Vogel O, Griewank A, Bär G. Direct gear tooth contact analysis for hypoid bevel gears. *Comput Meth Appl Mech Eng* 2002;**191**: 3965–82.
25. Fang Z, Wei B, Deng X. Loaded tooth contact analysis for spiral bevel gears considering edge contact. In: *Proceedings of 11th world congress in mechanism and machine science*, Tianjin; 2004. p. 838–42.
26. Litvin F, Fuentes A, Hayasaka K. Design, manufacture, stress analysis, and experimental tests of low-noise high endurance spiral bevel gears. *Mech Mach Theory* 2006;**41**:83–118.
27. de Vaujany JP, Guingand M, Remond D, Icard Y. Numerical and experimental study of the loaded transmission error of a spiral bevel gear. *ASME J Mech Des* 2007;**129**:195–200.
28. Zhang J, Fang F, Cao X, Deng X. The modified pitch cone design of the hypoid gear: manufacture, stress analysis and experimental tests. *Mech Mach Theory* 2007;**42**:147–58.
29. Schlecht B, Schaefer S, Hutschenreiter B, Schropp S. Complex tooth contact analysis of bevel and hypoid gears involving load spectra. In: *Proceedings of international conference on gears*, Munich: VDI-Berichte 2108.2; 2010. p. 1321–35.
30. Wang PY, Fan SC, ZHuang ZG. Spiral bevel gear dynamic contact and tooth impact analysis. *ASME J Mech Des* 2011;**133**, 084501-1-6.
31. Simon V. Load distribution in hypoid gears. *ASME J Mech Des* 2000;**122**:529–35.
32. Simon V. Load distribution in spiral bevel gears. *ASME J Mech Des* 2007;**129**:201–9.
33. Simon V. Head-cutter for optimal tooth modifications in spiral bevel gears. *Mech Mach Theory* 2009;**44**:1420–35.
34. Piazza A, Vimercati M. Experimental validation of a computerized tool for face hobbed gear contact and tensile stress analysis. In: *Proceedings of 10th ASME international power transmission and gearing conference*, Las Vegas. Paper No. DETC2007/PTG-35911; 2007. p. 1–8.
35. Saiki K, Tobisawa K, Kano M, Ohnisi Y, Kusaka T. Loaded TCA of measured tooth flanks for lapped hypoid gears. In: *Proceedings of 10th ASME international power transmission and gearing conference*, Las Vegas. Paper No. DETC2007/PTG-34102; 2007. p. 1–6.
36. Nishino T. Generation and curvature analysis of face-hobbed hypoid gears. In: *Proceedings of JSME international conference on motion and power transmissions*, Sendai; 2009. p. 64–9.
37. Kolivand M, Kahraman A. A load distribution model for hypoid gears using ease-off topography and shell theory. *Mech Mach Theory* 2009;**44**:1848–65.
38. Kolivand M, Kahraman A. An ease-off based method for loaded tooth contact analysis of hypoid gears having local and global surface deviations. *ASME J Mech Des* 2010;**132**:071004.
39. Kawasaki K, Tsuji I. Analytical and experimental tooth contact pattern of large-sized spiral bevel gears in cyclo-palloid system. *ASME J Mech Des* 2010;**132**:041004.
40. Hotait M, Kahraman A, Nishino T. An investigation of root stresses of hypoid gears with misalignments. *ASME J Mech Des* 2011;**133**:071006.
41. Simon S. Influence of tooth modifications on tooth contact in face-hobbed spiral bevel gears. *Mech Mach Theory* 2011;**46**:1980–98.
42. Simon V. Deformations and stresses in face-hobbed spiral bevel gears. In: *Proceeding of the 11th ASME international power transmission and gearing conference*, Washington. Paper No. DETC2011/PTG-47089; 2011. p. 81–91.


**Vilmos Simon** is a professor at the Budapest University of Technology and Economics. His main research interests include geometry, kinematics, dynamics, manufacture and elastohydrodynamic analysis of lubrication in spur, helical, spiral bevel, hypoid, and cylindrical and globoidal (double enveloping) worm gears; development of finite element programs for the calculation of stresses and displacements in machine elements, especially in gears; elastohydrodynamic lubrication based design of rider rings; computer aided design and manufacture of cutting tools, especially tools for gear manufacture.